Dynamics and Internal Control of Body Temperature in Response to Infectious Agents and other Causal Factors

Charles D. Schaper, Ph.D.*

March 3, 2019

Abstract

Thermoregulation is crucial to homeostasis but the mechanisms by which body temperature is controlled are still largely mysterious, especially in response to infectious agents and other exogenous stressors. This research develops a model of body temperature dynamics with a new hypothesis of integrated pathways associated with the cardiovascular and nervous system. For the first time, chemical and neural signals are coordinated to mathematically characterize body temperature dynamics. Quantitative insight and model predictive capability for the dynamics and internal control of body temperature is developed in which a feedback-only controller is newly introduced. Further, the proposed multivariable feedback controller, is comprised of a superposition of proportional responses to signals and its rate of change in association with cardiovascular and neural pathways and is thus evaluated in a framework of linear equations to form a closed-loop model of body temperature control effects in response to causal factors, including those associated with the immune response. The model is validated by examination of the transient and spectral characteristics of a three-day case history involving temperature trajectories after routine exercise protocols inducing chills then fever in response to an initial standard vaccine injection of pneumococcal and influenza species. In addition, the model is applied to address and mathematically explain intriguing questions of thermoregulation, such as the mathematical description of fevers induced by infections, why chills often precede fever, and that fevers are due to a trade-off of robustness in favor of performance. The model is a comprehensive integration coordinating the cardiovascular and neural physiological systems to analyze, predict, and thereby produce regulation strategies to minimize body temperature deviations, especially in the presence of infections which are shown to fundamentally alter the inherent dynamic modes of the closed-loop temperature response.

*charlesschaper@comcast.net

Graphical Abstract

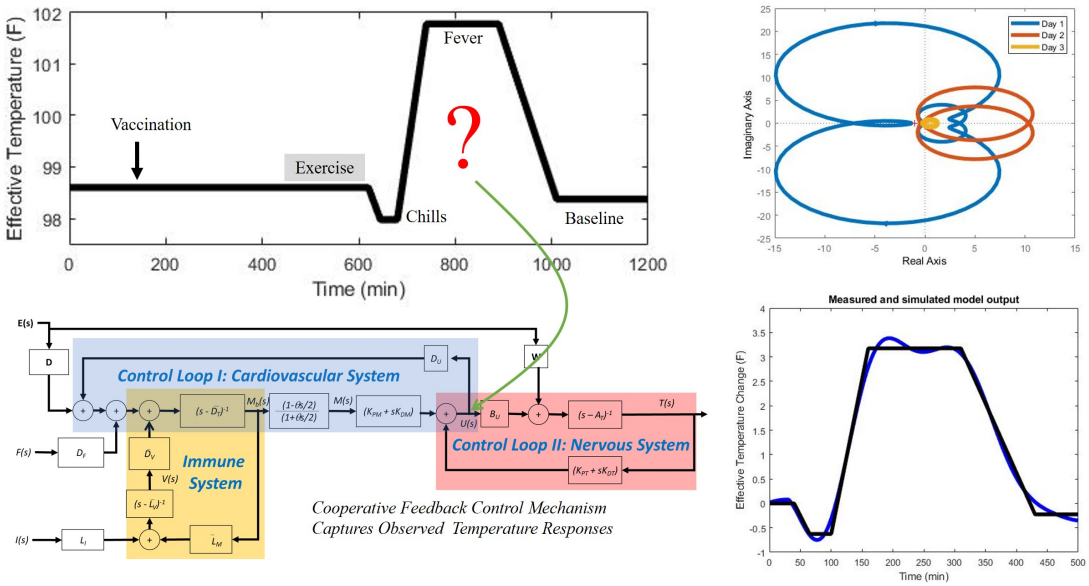

1 Introduction

Body temperature, despite its obvious importance to well-being and homeostasis, is surprisingly not well understood in terms of the underlying mechanisms and control laws that enable its high performance relative to large variations in environmental conditions [23]. Mathematical models unfortunately are not available that characterize observable temperature trajectories deviating from nominal conditions, for example chills preceding fevers in response to infections. Certainly on a general level, analytic insight to characterize body temperature would be useful for the caregiver and even on an individual level as deviations especially in relation to fever are always of the utmost concern. Furthermore, body temperature control needs to be very well understood as it is a symptom of an infection and other medical problems, indicative of its status and stage of curative progress; for example, almost all with cancer will have fever, the most common symptom of HIV is fever, and in contagious infections as chills are common to those with pneumonia.

Historically, the theory most popular for explaining temperature control, which is even currently taught in medical physiology textbooks [17] and referenced for the public in Wikipedia [11] as well as general scientific magazines [3] over decades, derives from an analogy to that of a thermostat, which supposedly is situated in the hypothalamus. This control law configuration proposes that the body in essence possesses an internal thermostat that compares a core temperature to an internal temperature setpoint, and based upon the error, issues thermoregulation commands, such as shivering, vasomotor action, and sweating, in order to bring to zero the deviation of core temperature and setpoint. Moreover, this historical theory proposes that the temperature setpoint can change from time-to-time; for example it suggests that when infected the setpoint of the thermostat is reset to a higher temperature, and thus the core body temperature will be controlled to the new higher level. Moreover, the theory suggests that fever is a defense mechanism, useful for fighting against infections because, as the theory indicates, some biological organisms perform poorer at the higher temperatures, and thus the body is trying to eliminate the infection by raising its internal temperature.

In the recent research literature, however alternative hypotheses for temperature control have been proposed which do away with the concept of a thermostat, since it has never been experimentally identified, and instead apply independent "thermoeffector loops" about balance points, thereby eliminating the need for setpoints and include concepts of feedforward control, in addition to feedback control [24]. Other research in thermoregulation is substantial, and includes many "bottoms-up" approaches, in which the chemistry of thermoceptors are sought that show cause and effect in relation to temperature, including mediators such as prostaglandin E2 [14] and proinflammatory cytokines [5], especially in relation to fever. In addition, neural circuits [29] are proposed of parallel efferent paths that have a common thermosensory input from the peripheral nervous system [21]. Still the methods by which control of temperature and the shapes of responses is still largely unknown [22].

Thus, an analytic basis for body temperature dynamics is not available and thus ques-

tions of commonly observed temperature effects are not satisfactorily answered, such as: Is fever "good or bad", that is, is fever actually a defense mechanism of infectious agents? Why does one even get a fever in the first place when infected? Why do chills often precede fever? For protocol following physical activity, what is the best way to control body temperature when infected with the flu? What role, if any, does feedforward have in body temperature control? Is there actually a temperature "set-point" for regulation that can be adjusted due to an infection, and if there is not a set-point, how is the temperature level established? In terms of performance, is the body temperature control system optimal or not, and if so, what is it optimized to do and what are the implications? This paper provides the internal control mechanisms, mathematical framework, and initial validation, from which to answer these questions and provide insight into the performance of body temperature control. Further, the intention is to not only develop the framework for such analysis, but also to enable predictive capability of temperature trajectories; and to give insight into the internal signals driving temperature, such as the dynamics of the neurological output from the temperature control system and the time varying concentrations expected of newly introduced chemical signals.

To develop this insight, a "top-down" approach to modeling is applied, in which a semi-empirical derivation of the basic equations surrounding temperature control, including its disturbances, are utilized, and of which a proposed control law is incorporated that enables the development of the closed-loop process. After derivation, the model structure is assessed for descriptive and predictive capability in validating its feasibility. As will be noted, several new ideas are utilized, and among the most critical is that of a chemical signal as a mediator molecule that not only characterizes the time-varying status of the cardiovascular system, such as its level of vasodilation, but which also imparts a temperature control function. Based on the research literature, such mediators are feasible, such as prostaglandins [7, 31, 1] or nitric oxide [25, 15, 30, 12, 10, 9], and that such mediators may also interact with the immune system in infectious response [26, 16, 6]. It is the intention to characterize the chemical mediator and its pathway, and to describe its characteristics from an input-output dynamic perspective, such that it will aid in its further identification.

At a high level, the approach developed in this paper is described by the schematic in Figure 1. An infectious component interacts with the mediator signal of the cardiovascular system, which is then transported to the central nervous system, where it interacts with the thermoreceptors to form a response signal that is implemented by thermoeffectors. The changes in body temperature results in a response to the thermoreceptors, and the changes necessary to induce the response in body temperature are also reflected in updates to the mediator signal within the cardiovascular system. This basic description is then expanded to include other factors besides infectious agents, such as inputs induced by physical activity or exercise, as well as other stressors inducing fight or flight response, and chemical inputs such as anti-pyretics. This research introduces for the first time a chemical species associated with the cardiovascular system as a controlling factor in temperature control, thereby establishing pathways of the neural and cardiovascular systems in an

analytic characterization of the febrile response.

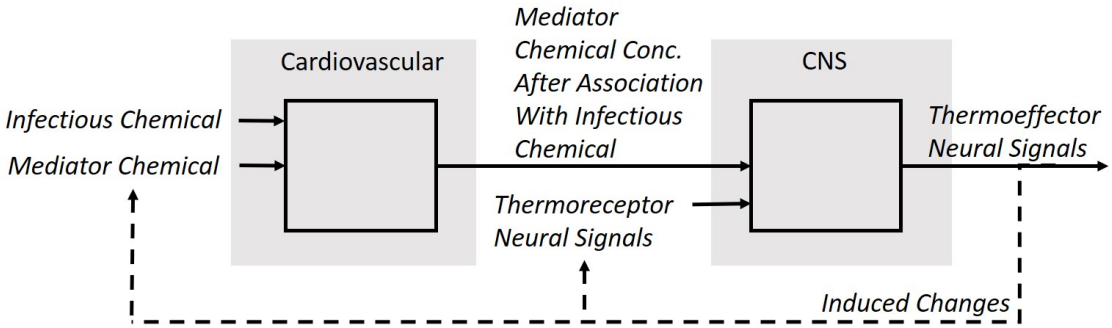

Figure 1: To clarify the new approach described herein, a simplified schematic is depicted as follows starting from the left: Mediator and Infectious agent chemically interact within the cardiovascular system, which thereby alters the concentration of the mediator from its nominal value. The mediator chemical is transported to the central nervous system and interacts with the neural signal associated with the thermoreceptors to generate signals associated with thermoeffectors, such as vasodilation or vasoconstriction. The thermoeffector signals then result in changes to the body temperature, which manifest in changes to both the thermoreceptors and the mediator concentration by the manipulations, such as vasodilation or vasoconstriction, that caused the adjustments in body temperature. In the manuscript, additional inputs to the cardiovascular are included to fully model the body temperature impact, such as anti-pyretics and stressors, such as those from physical activity or exercise.

To develop an approach of understanding body temperature control in response to an infectious agent that triggers deviation, a mathematical model of body temperature control is first developed. To test its validation, a case study is produced in which a routine protocol was followed in physical activity, exercise, whose only difference was an administration of a pneumococcal agent earlier in the day, which induced a febrile response through the lipopolysaccaride material. The model is examined for its predictive capability by examining its internal structure in characterizing the observed temperature trajectories. The model can then be further examined to provide an answer to the questions raised earlier concerning fever, chills, and other matters. Although temperature control is complex, the resulting mode provides insights and predictive capabilities, as well as a coordinated framework for the cardiovascular, nervous, and immune systems in terms of temperature; thus, the model should contribute significantly to the understanding of body temperature control.

2 Methods

To develop a quantitative analysis of internal control mechanisms for body temperature, a "top-down" approach is deployed that derives a model based on linear approximations of closed-loop dynamics of time-varying responses consistent with observable measurements. The resultant model is a lumped parameter structure that can be identified from input-output data and validated by its analysis and predictive capability, as well as its internal structure An important aspect of this analysis is the temperature control law postulated, as it will determine its overall integration and coordination within the network of systems, and its interaction with causal factors, including infectious agents and internal stimulation.

2.1 Temperature Control Law

To quantify the dynamics and control of body temperature, a mechanism is proposed by which a control output response is generated from input signals, both neurological and chemical, that establish physical status as it pertains to temperature. An insight offered by this paper is the introduction of a mediator signaling which correlates to an effective temperature response. As pointed out in the introduction, the source of this signal may be, for example, associated with prostaglandin, nitric oxide, or similar molecule from which the control output is generated in proportion to its deviation from nominal and to its accompanying rate of change. Hence, with the superposition with the neural signals associated with temperature and its rate of change and the concentration of the mediator chemical signal and its rate of change, the control law by which temperature compensation is made is postulated as follows:

$$U = f(T, M, \dot{T}, \dot{M}) \tag{1}$$

where U is the manipulated signal to the temperature control system, T denotes an effective temperature associated with the body, M is the chemical signal indicating the status of the response induced by the manipulated input, $\dot{T} \equiv dT/dt$ and $\dot{M} \equiv dM/dt$, which are the rates of change associated with the temperature and chemical responses.

The rationale for incorporating the rate of change as a signal of the internal controller is that the concentration gradient at the synaptic cleft will define the speed and amplitude of the temperature response. The concentration gradient is associated with an open system and subject to second order partial differential equations of a flow fields, such as that of the Navier-Stokes formulation. The boundary conditions associated with such models take into account the spatial gradient, and the time derivative associated with the input of M and T to the introduction of the axonal receptors will establish the spatial concentration gradient.

A schematic of the control law, which is determined in the central nervous system, is depicted in Figure 2 in which the linkage with the cardiovascular system is also shown for

clarity, including the infectious agent V and body concentration of the mediator signal M_b, which are described in subsequent sections.

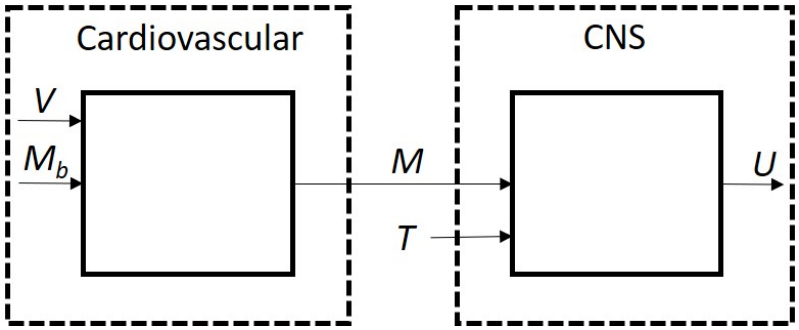

Figure 2: A schematic of the control law focuses on the input-output relation of the central nervous system (CNS), but it is noted for completeness that the signal entering the CNS, M, which represents the concentration of the mediator signal, is associated with the cardiovascular system in which it undergoes association or reaction with the infectious agent V. The temperature is represented as a neural signal T and the output from the CNS is U which is a neural signal associated with the interaction of the synaptic cleft of M and T. The mediator M can cross between the blood-brain barrier in order to produce such changes, thereby linking the cardiovascular and nervous system in terms of temperature control. The output signal undergoes further processing to produce thermoeffector signals. Later, other inputs to the cardiovascular system which input the concentration of the mediator signal M_b are included.

The effective temperature T is one that need not be explicitly measured, but rather a signal that is representative of body temperature, which can be obtained from a combination of thermoreceptors. The output of the manipulated neural signal, U, may signify a combination of responses to the system, such as increase or decrease in vasodilation, sweating, shivering, and other such mechanisms employed to control temperature. For the purposes of this study, the distribution of the output signal to the effector mechanisms is secondary to the analysis and can be taken-up for study as it will not impact the present analysis. Thus, to obtain a mathematical representation of the control law, a Taylor Series expansion [28] of Equation (1) is taken about a nominal operating point denoted as U_0, T_0, M_0, which would be associated with a standard body temperature, and truncated after the first term results in the expression,

$$U = f(T_0, M_0, \dot{T}_0, \dot{M}_0) + K_{pT}(T - T_0) + K_{dT}(\dot{T} - \dot{T}_0) + K_{pM}(M - M_0) + K_{dM}(\dot{M} - \dot{M}_0) \quad (2)$$

of which the control law scaling factors, which are critical in its performance, are given by:

$$K_{pT} = \frac{\partial f(T, M, \dot{T}, \dot{M})}{\partial T}\Big|_{\substack{T=T_0, \dot{T}=\dot{T}_0 \\ M=M_0, \dot{M}=\dot{M}_0}} \tag{3}$$

$$K_{dT} = \frac{\partial f(T, M, \dot{T}, \dot{M})}{\partial \dot{T}}\Big|_{\substack{T=T_0, \dot{T}=\dot{T}_0 \\ M=M_0, \dot{M}=\dot{M}_0}} \tag{4}$$

$$K_{pM} = \frac{\partial f(T, M, \dot{T}, \dot{M})}{\partial M}\Big|_{\substack{T=T_0, \dot{T}=\dot{T}_0 \\ M=M_0, \dot{M}=\dot{M}_0}} \tag{5}$$

$$K_{dM} = \frac{\partial f(T, M, \dot{T}, \dot{M})}{\partial \dot{M}}\Big|_{\substack{T=T_0, \dot{T}=\dot{T}_0 \\ M=M_0, \dot{M}=\dot{M}_0}} \tag{6}$$

Deviation variables are defined as $\Delta U = U - U_0$, $\Delta T = T - T_0$, $\Delta M = M - M_0$, and thus we have the control law expressed after substitution into Equation (2) as

$$\Delta U = K_{pT}\Delta T + K_{dT}\Delta\dot{T} + K_{pM}\Delta M + K_{dM}\Delta\dot{M} \tag{7}$$

It is noted that the control law, Equation (7), is considered as having a PD (proportional-derivative) form, which is deployed in industrial process control with success. The proportional terms provide a means of using a feedback control mechanism to manipulate the input variable so as to steer the controlled signals about a nominal value. The derivative terms is primarily to shape the response to desirable trajectories, for example speeding-up the control action, but does not in general influence the stability of the system. Industrial controllers have benefitted from an integrating action, in which the error in the control signal is driven ultimately to zero; however it does introduce instability and there is no evidence that an integrating action is incorporated.

As indicated, one of the key contributions of this analysis is the incorporation of a feedback mechanism based on a chemical signal that indicates the status of the response to the input signal, which could be, for example, in response to a vasodilation or vasoconstriction commands that regulate temperature response. Moreover, based on observable responses to infectious agents, it appears mandatory to incorporate such a coupling mechanisms, since without it, and a feedback controller that just fed back on temperature would not be able to capture the impact of infectious agents, which is experimentally observable as will be discussed in the validation example of Section 3.

2.2 Model of Temperature Dynamics

The temperature by which control signals are generated according to the control law of Equation (7) corresponds to an effective signal that is expressed as a function shown in Equation (8), which is comprised of not only variables T and U, but also exogeneous inputs, $[E_1, E_2, \ldots, E_n]$ that can have effect on body temperature, such as exercise, clothing,

environmental factors of humidity and temperature, infrared heating, and other inputs including stressors such as those associated with deviations of the sympathetic and parasympathetic nervous system, and thus $E_j(s)$ can incorporate inputs due to emotional stress, cerebral thoughts that may induce sympathetic activity, torpor, hibernation and other activities associated with parasympathetic activity. Open-loop expressions of temperature models, which are first order, and its influence from external factors such as drugs and exercise have been developed [4]. In the approach developed in this paper, the representation for temperature is developed in closed-loop format for general sets of inputs. As the body temperature is in general non-uniform, the temperature of concern here is an "effective" temperature, that is one in which the control laws ultimately respond after integration of the neurological thermoreceptors. The effective temperature dynamics are expressed as

$$\frac{dT}{dt} = g(T, U, E_1, E_2, \ldots, E_n) \tag{8}$$

A linear dynamic model is obtained from a Taylor Series expansion of Equation (8) and then neglecting all terms of order two and higher, to arrive at the expression:

$$\frac{dT}{dt} = g(T_0, U_0, E_{1,0}, E_{2,0}, \ldots, E_{n,0}) + A_T(T - T_0) + B_U(U - U_0) + \sum_{j=1}^{n} W_j(E_j - E_{j,0}) \tag{9}$$

where the model parameters are found from:

$$A_T = \frac{\partial g(T, U, E_1, E_2, \ldots, E_n)}{\partial T}\Big|_{\substack{T=T_0, U=U_0 \\ E_l=E_{l,0}, l=1,\ldots,n}} \tag{10}$$

$$B_U = \frac{\partial g(T, U, E_1, E_2, \ldots, E_n)}{\partial U}\Big|_{\substack{T=T_0, U=U_0 \\ E_l=E_{l,0}, l=1,\ldots,n}} \tag{11}$$

$$W_j = \frac{\partial g(T, U, E_1, E_2, \ldots, E_n)}{\partial E_j}\Big|_{\substack{T=T_0, U=U_0 \\ E_l=E_{l,0}, l=1,\ldots,n}} \tag{12}$$

Utilizing deviation variable format with $\Delta E_j = E_j - E_{0,j}$ about a nominal level, which could be 0, an expression for the temperature dynamics is achieved:

$$\frac{d\Delta T}{dt} = A_T \Delta T + B_U \Delta U + \sum_{j=1}^{n} W_j \Delta E_j \tag{13}$$

Equation (13) is a linearized model which maps the temperature state trajectories, inputs from the control law, and exogeneous inputs to changes in temperature, and is typical of the dynamic response of thermal systems when used for control system analysis about nominal operating windows.

2.3 Reporter Signal Dynamics

In this paper, in the development of the feedback control law of temperature, it is proposed that a chemical species, which is indicative of the status of the effects of the controller output signal in its response to temperature, such as measurable by bloodstream molecules. It is further proposed that this reporter signal is reactive with external agents, such as infectious components or vaccines, and whose rate of reaction is defined as R, and thus the agent interferes with the control signal. Further the external inputs to the system are considered to be potentially influential on the reporter signal dynamics, such as the effects of exercise. Also incorporated is the potential for an external feed stream F that can provide an external source of reporter signal molecules, or one in which can be used to control temperature, such as an antipyretic. The resulting function is expressed therefore as follows:

$$\frac{dM_b}{dt} = h(M_b, U, R, E_1, E_2, \ldots, E_n, F) \tag{14}$$

and in producing a linearized representation of Equation (14), a Taylor Series expansion truncated after the first term yields:

$$\frac{dM_b}{dt} = h(M_{b,0}, U_0, R_0, E_{1,0}, E_{2,0}, \ldots, E_{n,0}, F_0) + D_M(M_b - M_{b,0}) + D_U(U - U_0) + D_R(R - R_0) + \sum_{j=1}^{n} D_j(E_j - E_{j,0}) + D_F(F - F_0) \tag{15}$$

where

$$D_M = \frac{\partial h(M_b, U, R, E_1, E_2, \ldots, E_n, F)}{\partial M_b}\Big|_{\substack{M_b=M_{b,0}, U=U_0, R=R_0, F=F_0 \\ E_l=E_{l,0}, l=1,\ldots,n}} \tag{16}$$

$$D_U = \frac{\partial h(M_b, U, R, E_1, E_2, \ldots, E_n, F)}{\partial U}\Big|_{\substack{M_b=M_{b,0}, U=U_0, R=R_0, F=F_0 \\ E_l=E_{l,0}, l=1,\ldots,n}} \tag{17}$$

$$D_R = \frac{\partial h(M_b, U, R, E_1, E_2, \ldots, E_n, F)}{\partial R}\Big|_{\substack{M_b=M_{b,0}, U=U_0, R=R_0, F=F_0 \\ E_l=E_{l,0}, l=1,\ldots,n}} \tag{18}$$

$$D_j = \frac{\partial h(M_b, U, R, E_1, E_2, \ldots, E_n, F)}{\partial E_j}\Big|_{\substack{M_b=M_{b,0}, U=U_0, R=R_0, F=F_0 \\ E_l=E_{l,0}, l=1,\ldots,n}} \tag{19}$$

$$D_F = \frac{\partial h(M_b, U, R, E_1, E_2, \ldots, E_n, F)}{\partial F}\Big|_{\substack{M_b=M_{b,0}, U=U_0, R=R_0, F=F_0 \\ E_l=E_{l,0}, l=1,\ldots,n}} \tag{20}$$

For the reaction rate R, we consider a reaction law which is dependent upon the concentration of the external reactive component V, such as a bacterial or viral vaccine, and the concentration of the reporter signal molecule:

$$R = h_R(V, M_b) \tag{21}$$

An example would be a second order reaction would be $R = k_{VM}VM$ with k_{VM} a rate constant. While the rate coefficients may be a function of temperature, it is considered that such effects will be secondary and thus can be neglected without loss of generality. Linearizing the reaction rate representation of Equation (21)yields:

$$R = R_0 + K_{MV}(M_b - M_{b,0}) + K_{VM}(V - V_0) \tag{22}$$

where

$$K_{VM} = \frac{\partial h_R(V, M_b)}{\partial V}\Big|_{\substack{V=V_0 \\ M_b=M_{b,0}}} \tag{23}$$

$$K_{MV} = \frac{\partial h_R(V, M_b)}{\partial M_b}\Big|_{\substack{V=V_0 \\ M_b=M_{b,0}}} \tag{24}$$

And thus the substituting Equation (21) into Equation (15), and utilizing deviation variables $\Delta F = F - F_0$ and $\Delta V = V - V_0$, the following equation for the reporter signal molecular is obtained,

$$\frac{d\Delta M_b}{dt} = \bar{D}_T \Delta M_b + D_U \Delta U + \sum_{j=1}^{n} D_j \Delta E_j + D_F \Delta F + \bar{D}_V \Delta V \tag{25}$$

where

$$\bar{D}_T = D_M + D_R K_{MV} \tag{26}$$

$$\bar{D}_V = D_R K_{VM} \tag{27}$$

Note that the temperature associated dynamics of the reporter signal molecule, $\bar{D}_T$ are influenced by the reaction kinetics K_{MV} of the external agent with the reporter molecule.

2.4 Invasive agent dynamic model

For the invasive agent V, its dynamic model is represented from a species balance as follows:

$$\frac{dV}{dt} = h_V(V, I, R) \tag{28}$$

where I is the mechanism by which the invasive agent enters the system, such as with an injection or internal incubation period subsequent to release. The model is also a function of the reaction rate R with the reporter signal molecule. A Taylor Series expansion truncated after the first term yields,

$$\frac{dV}{dt} = h_V(V_0, I_0, R_0) + L_V(V - V_0) + L_I(I - I_0) + L_R(R - R_0) \tag{29}$$

where

$$L_V = \frac{\partial h_V(V, I, R)}{\partial V}\Big|_{V=V_0, I=I_0, R=R_0} \tag{30}$$

$$L_I = \frac{\partial h_V(V, I, R)}{\partial I}\Big|_{V=V_0, I=I_0, R=R_0} \tag{31}$$

$$L_R = \frac{\partial h_V(V, I, R)}{\partial R}\Big|_{V=V_0, I=I_0, R=R_0} \tag{32}$$

Substituting for Equation (21) R and taking deviation variables, $\Delta I = I - I_0$, yields

$$\frac{d\Delta V}{dt} = \bar{L}_V \Delta V + L_I \Delta I + \bar{L}_M \Delta M_b \tag{33}$$

where

$$\bar{L}_V = L_R K_{VM} \tag{34}$$

$$\bar{L}_M = L_R K_{MV} \tag{35}$$

2.5 State-space representation of dynamics

To form the system response of Equations (13), (25),(33), the state variables are defined as $\mathbf{\Delta X} = [\Delta T \Delta M_b \Delta V]^T$ and the disturbance variables as $\mathbf{Z} = [\Delta E_1 \Delta E_2 \ldots \Delta E_n \Delta F \Delta I]^T$ which can be related in state-space representation

$$\frac{d\mathbf{\Delta X}}{dt} = \mathbf{A_X \Delta X} + \mathbf{B_U} \Delta U + \mathbf{B_Z \Delta Z} \tag{36}$$

with the system matrices,

$$\mathbf{A_X} = \begin{bmatrix} A_T & 0 & 0 \\ 0 & \bar{D}_T & \bar{D}_V \\ 0 & \bar{L}_M & \bar{L}_V \end{bmatrix} \tag{37}$$

$$\mathbf{B_U} = \begin{bmatrix} B_U \\ D_U \\ 0 \end{bmatrix} \tag{38}$$

$$\mathbf{B_Z} = \begin{bmatrix} W_1 & W_2 & \ldots & W_n & 0 & 0 \\ D_1 & D_2 & \ldots & D_n & D_F & 0 \\ 0 & 0 & \ldots & 0 & 0 & L_I \end{bmatrix} \tag{39}$$

This state-space form has the general solution [18],

$$\mathbf{\Delta X}(t) = \int_0^t e^{\mathbf{A_X}(t-\tau)}\mathbf{B_U}\Delta U(\tau)d\tau + \int_0^t e^{\mathbf{A_X}(t-\tau)}\mathbf{B_Z}\mathbf{\Delta Z}(\tau)d\tau \tag{40}$$

The response, depending upon the nature of the system matrices, is in general comprised of a series of attenuated trigonometric oscillating functions, which in general does exhibit consistency with observed temperature responses especially in fever.

2.6 Time Delay

The location of the control response to the concentration of the reporter signal may be distinct relative to that of the local anatomical sectors responsible for its generation, and thus the transportation delay is modeled by a time delay function:

$$M(t) = M_b(t - \theta_M) \tag{41}$$

In similar fashion, the effective temperature utilized by the feedback control law could be modeled with a similar delay function, but it will be slower for a neurological input source, and thus for the present purposes, it is not incorporated.

2.7 Dynamic System Response

In forming a set of linear, time-invariant models to describe the closed-loop temperature dynamics, the LaPlace transform of Equations (7), (13), (25),(33) is taken, in $U(s) = \mathcal{L}[\Delta U]$, $T(s) = \mathcal{L}[\Delta T]$, $M(s) = \mathcal{L}[\Delta M]$, $V(s) = \mathcal{L}[\Delta V]$, $F(s) = \mathcal{L}[\Delta F]$, $I(s) = \mathcal{L}[\Delta I]$, $M_b(s) = \mathcal{L}[\Delta M_b]$, $E_j(s) = \mathcal{L}[\Delta E_j]$

$$U(s) = (K_{pT} + sK_{dT})T(s) + (K_{pM} + sK_{dM})M(s) \tag{42}$$

$$sT(s) = A_T T(s) + B_U U(s) + \sum_{j=1}^{n} W_j E_j(s) \tag{43}$$

$$sM_b(s) = \bar{D}_T M_b(s) + D_U U(s) + \sum_{j=1}^{n} D_j E_j(s) + D_F F(s) + \bar{D}_V V(s) \tag{44}$$

$$sV(s) = \bar{L}_V V(s) + L_I I(s) + \bar{L}_M M_b(s) \tag{45}$$

For the time delay Equation (41), the representation in LaPlace transform is given by

$$M(s) = e^{-\theta s} M_b(s) \tag{46}$$

And using the Padé approximation [27] for the time delay term, which results in

$$e^{-\theta s} = \frac{1 - \frac{\theta}{2}s}{1 + \frac{\theta}{2}s} \tag{47}$$

The closed-loop schematic representation of Equations (42), (43), (44), (45), and (47) is presented in the block diagram of Figure 3, which maps the inputs to the system $E(s)$, $I(s)$, $F(s)$ to the output temperature signal $T(s)$. The internal control loop is highlighted indicating the intersection of two coordinated control loops, which will be discussed further in Section 4.

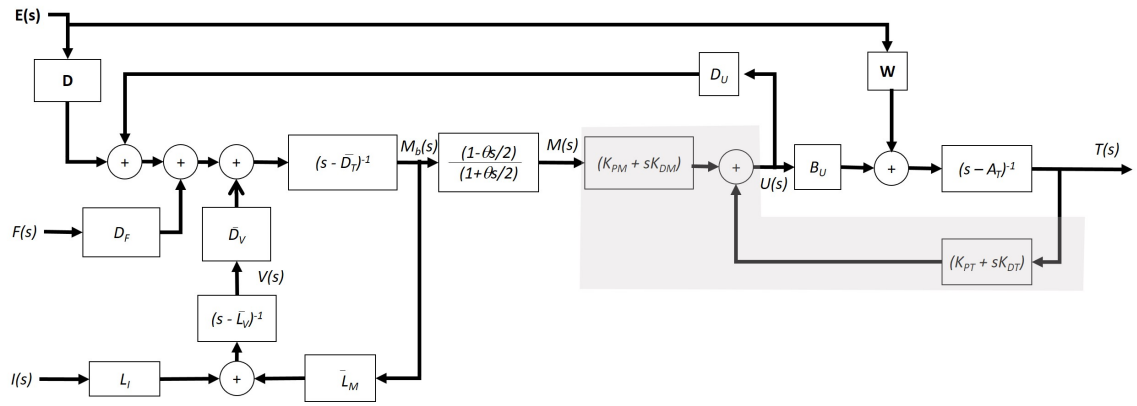

Figure 3: The block diagram of the closed-loop response to temperature in response to inputs from infectious agents $V(s)$, from external pyrogenic agents $F(s)$, and from a vector of external sources, $\mathbf{E}(s)$, which comprise rigorous exercise and other such physical activity, as well as other external stressors and temperature inducing behavioral factors. The blocks comprise the transfer functions of the model, and include the control law function for $U(s)$ which comprises feedback from body temperature $T(s)$ and a mediator that acts as a status indicator $M(s)$, as shown by the shaded region. This block diagram will be further evaluated in Section 4 by partitioning into sectors demonstrating the integration of the nervous, cardiovascular and immune systems.

2.8 LTI Models at Multiple Operating Points

To arrive at the final set of equations to describe the dynamic response and internal control operations of body temperature, a subscript k is appended to the model relations to indicate that the approximations of the functionals describing system performance are linearized and that the nonlinear behavior of the system is characterized by a sequence of LTI models taken around a nominal operating point. In the development of this approach, the output units of interest in characterizing the response are represented as follows:

$$\mathbf{Y}(s) = \begin{bmatrix} T(s) \\ U(s) \\ M(s) \end{bmatrix} \tag{48}$$

$$\mathbf{Z}(s) = \begin{bmatrix} E_1(s) \\ E_2(s) \\ \vdots \\ E_n(s) \\ F(s) \\ I(s) \end{bmatrix} \tag{49}$$

At the linearization point denoted as $k = 1, 2, \ldots, r$ for a series of r LTI models in which an indvidual operating point is given by:

$$\mathbf{G_k^c}(s) = \begin{bmatrix} G^c_{TE,1k} & G^c_{TE,2k} & \ldots & G^c_{TE,nk} & G^c_{TF,k}(s) & G^c_{TI,k}(s) \\ G^c_{UE,1k} & G^c_{UE,2k} & \ldots & G^c_{UE,nk} & G^c_{UF,k}(s) & G^c_{UI,k}(s) \\ G^c_{ME,1k} & G^c_{ME,2k} & \ldots & G^c_{ME,nk} & G^c_{MF,k}(s) & G^c_{MI,k}(s) \end{bmatrix} \tag{50}$$

$$\mathbf{Y}(s) = \mathbf{G_k^c}(s)\mathbf{Z}(s) \tag{51}$$

and the closed-loop matrix are specified as,

$$G^c_{TE,jk}(s) = h_2^{-1}(s)(D_j h_1(s) + W_j) \tag{52}$$

$$G^c_{TF,k}(s) = h_2^{-1}(s) h_1(s) D_E \tag{53}$$

$$G^c_{TI,k}(s) = h_2^{-1}(s) \frac{h_1(s)\bar{D}_V L_I}{(s - \bar{L}_V)} \tag{54}$$

$$h_1(s) = \left[\frac{(s - \bar{D}_T)(1 + \frac{\theta}{2}s)}{(1 - \frac{\theta}{2}s)} - D_U(K_{pM} + sK_{dM}) - \frac{\bar{L}_M}{(s - \bar{L}_V)} \frac{(1 + \frac{\theta}{2}s)}{(1 - \frac{\theta}{2}s)} \right]^{-1} \tag{55}$$

$$h_2(s) = (s - A_T) - B_U(K_{pT} + sK_{dT}) - B_U(K_{pM} + sK_{dM}) h_1(s) D_U(K_{pT} + sK_{dT}) \tag{56}$$

$$G^c_{UE,jk}(s) = \frac{(s - A_T)G^c_{TE,jk}(s) - W_j}{B_U} \tag{57}$$

$$G^c_{UF,k}(s) = \frac{(s - A_T)G^c_{TF,k}(s)}{B_U} \tag{58}$$

$$G^c_{UI,k}(s) = \frac{(s - A_T)G^c_{TI,k}(s)}{B_U} \tag{59}$$

$$G^c_{ME,jk}(s) = \frac{G^c_{UE,jk}(s) - (K_{pT} + sK_{dT})G^c_{TE,jk}(s)}{(K_{pM} + sK_{dM})} \tag{60}$$

$$G^c_{MF,k}(s) = \frac{G^c_{UF,k}(s) - (K_{pT} + sK_{dT})G^c_{TF,jk}(s)}{(K_{pM} + sK_{dM})} \tag{61}$$

$$G^c_{MI,k}(s) = \frac{G^c_{UI,jk}(s) - (K_{pT} + sK_{dT})G^c_{TI,jk}(s)}{(K_{pM} + sK_{dM})} \tag{62}$$

The set of model equations describing the temperature control system about operating points $\mathbf{G^c}(s)$ is thus represented as

$$\mathbf{G^c}(s) = \{\mathbf{G^c_k}(s) : k = 1, 2, \ldots, r\} \tag{63}$$

3 Results

To assess the analysis and predictive capability of the closed-loop model, including its proposed feedback control law mechanism, a case file of temperature fluctuations is examined in which such dynamics were observed due to a vaccination injection followed by rigorous exercise at regular intervals over a multiple daily period. If the model is to describe the dynamics, its fundamental pole-zero structure should track the observed temperature data and adequately fit the main modes of the trajectory data. The following case is studied:

Case History: A participant in excellent health (Pulse rate: 45 bpm; Weight 181 pounds; Waist-to-Height Ratio 0.44; Blood Pressure 123/72; Oral Temperature 97.5°F; Cholesterol 128 mg/dL (Standard Range <= 239 mg/dL); LDL 29 mg/dL (<= 159 mg/dL); HDL 74 mg/dL (>= 40 mg/dL); WBC Count 5.0 K/uL (3.7 - 11.1 K/uL); RBC Count 4.36 M/uL (4.10 - 5.70 M/uL); Hematocrit 41.7% (39.0 - 51.0%); Hgb (14.6 g/dL (13.0 - 17.0 g/dL); MCV 96 fL (80 - 100 fL); RDW, RBC (11.9% (12.0 - 16.5%), Platelets 172 K/uL (140 - 400 K/uL), RBC's nucleated 0/100 WC) was administered by injection a vaccination associated with pneumococcal and influenza species prevention at approximately noon. The participant's temperature was reported as constant prior and immediately after the vaccination shots, and throughout a two-hour period of exercise that took place six hours after the injections. (This exercise routine had been repeated daily for a month preceding the vaccination.) Approximately ten minutes after completing the exercise period, which consisted of moderate weight training and a seven-mile jog on a treadmill, the participant reported the sensation of severe chills that lasted approximately forty minutes followed by a rapid rise in temperature to a nominal fever, which lasted two hours, followed by sweats in a return to a baseline temperature, thereby concluding the episode seven hours after the completion of the exercise period. The participant reported feeling fine after the episode of temperature fluctuation. On Day 2 and on Day 3, following the same exercise protocol at the same time of day, the participant reported a similar response in temperature response, through much less severe, of which the intensity of the response was estimated as level 8, 3, and 1 for each of the three days, and the period of response was longer during the chill period but shorter in time at the higher temperatures. The first day required bed rest during the seven hours of high temperature excursion to deal with the chills and fever, while the second and third day did not require bed rest. By the fourth day, no adverse temperature effects were felt following the exercise protocol of a seven mile jog. The response is characterized in Table 1. It was noted that for the pneumococcal vaccine, similar experiences of chills followed by fever were reported from on-line patient feedback, hence the display of temperature effects following vaccination was deemed to be fairly typical, although this case was particularly well characterized as the exercise regimen was a precursor to a significant dynamic temperature response.

Day	ΔT_{chill}	ΔT_{fever}	Δt_{chill}	Δt_{fever}	$\Delta t^{\text{ramp}}_{\text{chill}}$	$\Delta t^{\text{ramp}}_{\text{fever}}$	$\Delta t^{\text{ramp}}_{\text{baseline}}$
1	$-0.62°$F	$3.2°$F	35 min	150 min	25 min	60 min	120 min
2	$-0.23°$F	$1.1°$F	20 min	60 min	70 min	120 min	120 min
3	$-0.08°$F	$0.4°$F	60 min	30 min	70 min	120 min	140 min

Table 1: The effective temperature change in response to vaccination and exercise over a three day period, of which the fourth day was a return to baseline. The response characteristics follow a 8:3:1 relative weighting among each day with the high temperature ΔT_{fever}*, low temperature* ΔT_{chill}*, time periods* Δt_{chill}*,* Δt_{fever} *and ramping periods completing the sequence* $\Delta t^{\text{ramp}}_{\text{chill}}$*,* $\Delta t^{\text{ramp}}_{\text{fever}}$*,* $\Delta t^{\text{ramp}}_{\text{baseline}}$ *.*

The motivation for configuring this procedure to study temperature dynamics is of several advantages: (1) Model identification has been successfully deployed by the implementation of so-called step-responses, in which a step excitation in the input is made, and the output dynamics are studied: a model is then fit to the data, for example see the textbook on process control in the chemical industries [27]. The use of the data immediately after completing a session of physical data can therefore be modeled as a step response in the input $E(s)$ and therefore the time constants can be clearly identified. (2) Because the exercise session was the normal routine, which had been repeated many times in previous days, at the same time, and under essentially the same *a priori* conditions, a clear response due to the impact of the vaccination could be realized. Since there were no changes to the normal routine, other than the vaccine injection, there was no other explanation for the trigger but the vaccine. (3) To one not engaged in exercise, a seven mile jog and half hour of weight training would seem rigorous; however, if it is routinely performed on a daily, it was done without much effort, and thus effects due to physical exertion could be ruled out. (4) The response of chill followed by fever is hypothesized in this research to be due to a cardiovascular signal not in-synchronization as usual with the neural signal associated with the temperature. Hence measuring temperature would not be enough to track the response. It has to be performed in which the patient can provide indication of the effects such as shivering and chill effects in order to quantify the response. Thus, through patient interview, a quantitative assessment of temperature dynamics based on prior experience

can be achieved. (5) By repeating the experiment over a multi-day period, the effect of lowered concentration of vaccine can be examined on the impact of the dynamic modes associated with the temperature response.

To quantify this response and evaluate the model and feedback control law, an effective temperature change trajectory was generated for each of the three days during the period of interest. The trajectories in which the effective temperature is quantified as based on prior experiences, are relative to each from day to day on the intensity ratio of 8:3:1. It is noted that the response is one in which the effective temperature that is induced actually is modeled as dropping in magnitude to reflect the experiences of the patient, and then followed by a rise to a fever pitch consistent with prior experiences, followed by a breaking of the fever with a return to baseline. While the actual temperature need not be measured, thus the data is considered to be an "effective temperature" and the key points of the analysis are the relative departure in amplitude from nominal conditions on multiple sequential days and the timing associated with the temperature trajectories. Since the patient performed the exercise for multiple days prior to the inoculation, the amplitude and time response from nominal could be well characterized for the routine. Thus, the model is scaled to reflect deviations from nominal conditions in which the time constants and associated dynamic characterization will be accurate and consistent with the model derivation. From this set of data points, a linear spline function is fit to the data points, which is then used as input to the system identification algorithm. The time scale for all analysis is performed in minutes, including the subsequent temporal and spectral characterization. The basal values of $M_0, T_0, \dot{M}_0, \dot{T}_0$ are selected as steady-state just prior to completing the exercise routine, and thus the excitation input to the system is the step transition from physical activity to no physical activity, which enters the model through $E(s)$.

To evaluate the ability of the model to produce the characteristic temperature response, a model for each of the three days is fit to the data using system identification techniques [19] available in the Matlab programming language with the forcing function of a step-down in $E_1(s)$ considered as the exogenous input of exercise activity. As consistent with the model derivation, the model order was selected as four poles and three zeros, and the mean square error was minimized in determining the model parameters. Using the multiple, linear time-invariant model representation about each new operating point, a model was produced for each of the three days. The temperature response were then plotted in comparison to the generated data as presented in Figure 4, which show agreement in mapping the inverse response corresponding to the temperature chills effect, followed by the temperature rise, either plateauing or momentarily hitting a peak, and then terminating from a cool-down to baseline temperature.

The models in Laplace transform format of the closed-loop system response, $\mathbf{G^c}(s)$ for each of the three days is listed in Table 2 including a goodness of fit metric, which is the normalized root mean square criterion, a measure of the capability of the model to reproduce the observed data relative to the mean of the data. The goodness of fit exceeds

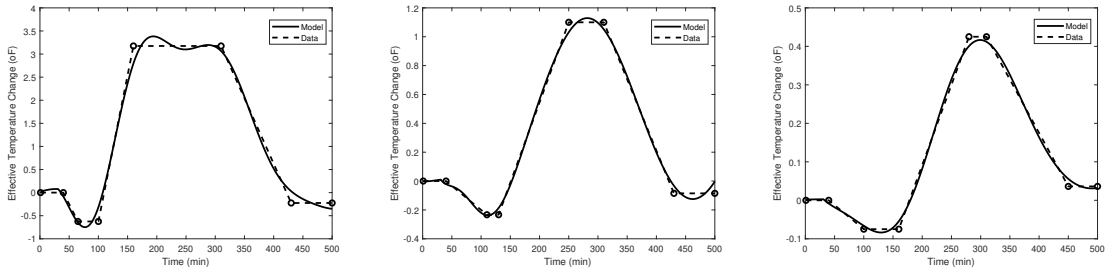

(a) Day 1 (b) Day 2 (c) Day 3

Figure 4: As an initial indication of model validation, a comparison of the measured and modeled trajectory of temperature is compared for each of the three days. The inverse dynamics of the model are clearly captured in showing a dip down in temperature followed by a rise and then a cool down back to base. For Day 1, some oscillation at the level off period in temperature is noted, while the static gains in settling the response for each of the days is indicated. Thus, the relatively close representation of the model output to that observed would indicate that the modeling approach is appropriate and that it can be examined for predictive and analysis capability.

90% for each of the three models, which typically is required to produce acceptable fits of the model to the data.

In assessment of the internal dynamics of the closed-loop models and the transition from day to day while the vaccine is removed by phagocytosis, the frequency response of the models for each of the three days is presented in Figure 5. For feedback control analysis, the frequency response is a useful indicator of the limits of performance [8]. It is noted that the second harmonic is strong on the first day, and then is less over the next two days. As the response curves tend to show a response closer to a single oscillatory function, one would expect a stronger magnitude at a single harmonic for Day 2 and Day 3, while on Day 1, the transition into a fever, which is held for some time, requires additional faster harmonic functions to model appropriately. The characteristics of the frequency response shows the static gain at low frequencies, and the resonant frequency indicates the peak response based upon the excitation of the input signal, which in this case is through rigorous exercise.

In Table 3, the location of the poles and zeros, as well as the gain margin and phase margin, of the identified closed-loop models is presented. It is noted that there is a right half plane zero for each of the models, which is indicative of the inverse response of chills preceding fever. The poles of the model are all negative, which is an indicative of stability, and the poles are of an imaginary number, indicating the oscillatory nature of the system response. The gain margin for Day 1 is negative, which means that if there was another feedback control law wrapped around this system response, it would be unstable. Day 2 and Day 3 have gain margins and phase margins consistent with stability.

Day	Model Fit	Closed-Loop Model $G^c(s)$
1	92.8%	$\frac{0.01276s^3+0.001238s^2-1.839e-05s-3.836e-07}{s^4+0.01148s^3+0.001893s^2+4.122e-06s+2.825e-07}$
2	95.4%	$\frac{0.005706s^3-0.0002954s^2+3.322e-05s-4.696e-07}{s^4+0.04177s^3+0.00365s^2+1.595e-05s+9.973e-07}$
3	94.8%	$\frac{0.001407s^3-2.516e-05s^2+3.173e-06s-3.735e-08}{s^4+0.01384s^3+0.001179s^2+6.037e-06s+2.242e-07}$

Table 2: The closed-loop models, whose structure order was derived by modeling, that map body temperature response to exercise, or activity, input, independent of the particular trajectory of input excitation. Thus, the temperature response to various scenarios can be predicted, and the internal dynamics of the body temperature control can be studied in response to differing concentrations of vaccines as it is cleared from the body. The goodness of fit parameter measures the ability to replicate the observed data relative to the mean of the data, with in exceeding 90% for each of the days indicating a good fit for system identification purposes.

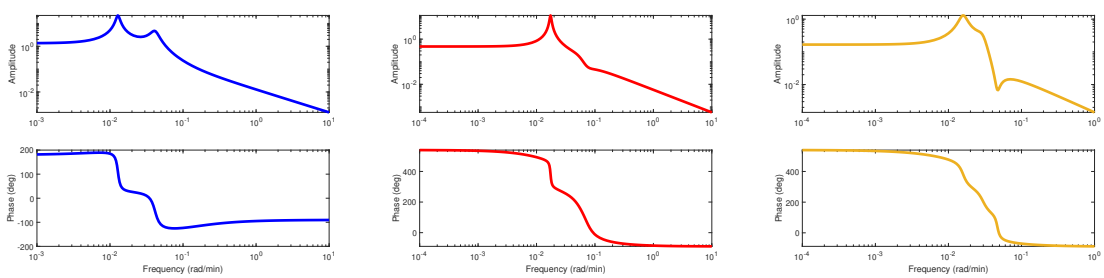

(a) Day 1 (b) Day 2 (c) Day 3

Figure 5: To characterize the types of responses in body temperature, the frequency response for each of the days is presented, which suggests that there are resonance modes that if matched or excited by the input, will result in significant deviation in temperature relative to other modes. This is useful as will be seen later in the paper on optimizing the input to the system in order to minimize fluctuation in temperature when infected. The shape of the curves are approximately the same from Day 1 to Days 2 and 3 as the vaccine is cleared, but the second resonant mode, which is associated with faster dynamic response, is reduced in amplitude, indicating a smoother trajectory represented by a single oscillatory state.

The Nyquist plot of the frequency response is presented in Figure 6 in comparing the

Day	Zeros	Poles	Gain Margin	Phase Margin
1	-0.1078 0.0229 -0.0122	$-0.0050 \pm 0.0411i$ $-0.0007 \pm 0.0128i$	-2.66, -17.1	58.6
2	$0.0181 \pm 0.0702i$ 0.0157	$-0.0203 \pm 0.0538i$ $-0.0006 \pm 0.0174i$	6.54, 14.4	-52.4, 99.1
3	$0.0029 \pm 0.0467i$ 0.0121	$-0.0049 \pm 0.0294i$ $-0.0020 \pm 0.0158i$	15.6, 13.1	-113, 153

Table 3: The dynamic characteristics of the Closed-Loop models for Day 1, 2 and 3 is compared. For each of the models, there is a zero located in the right half plane, which indicates that it is non-minimum phase and for a step input the output trajectory will follow an inverse response, in which the effective temperature will drop before it rises, that is chills before fever. The poles are imaginary numbers, which indicates that the response will contain oscillatory response modes as it is closer to instability. The margins indicate are adquate for Days 2 and 3 indicating robustness to disturbances, but for Day 1, it indicates lack of margin, and the response will be the most severe as the dynamics border instability.

dynamics of Day 1, Day 2, and Day 3, as the body transitions higher concentrations of the vaccine to lower concentrations as it is depleted. The vaccine is seen to have a significant effect on the dynamic response, and based on the Nyquist stability criteria involving the encirclement of the point $(-1, 0)$, would result in an unstable system if utilized with an additional layer of feedback control. Clearly, while infected the temperature dynamics are significantly compromised.

4 Discussion

As presented in Section 3, the proposed control law, which utilizes a feedback-only mechanism on the temperature and reporter signals, adequately models the observed temperature responses to external stressors for the case history of the observed temperature phenomena in the presence of vaccines. In this section, to further validate the model and demonstrate the insight provided by a mathematical characterization of the temperature response, the model structure is examined in additional detail to assess its ability to explain and to

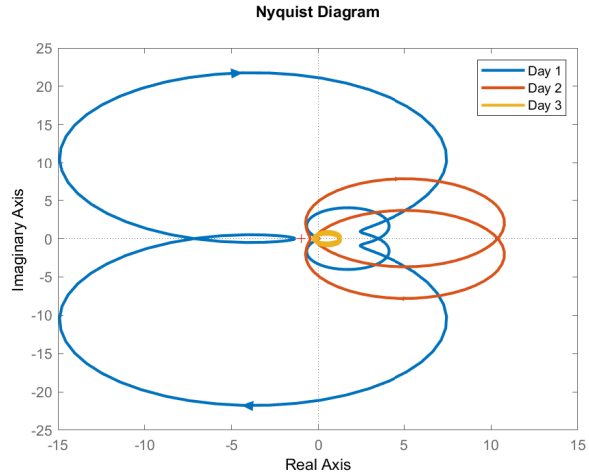

Figure 6: In evaluating the impact of the vaccine on body temperature control, the Nyquist representation of the models for Day 1, 2, and 3 is compared to show dramatically the severe degradation of temperature control due to the influence of the polysaccharide on the internal dynamics. The Nyquist plot shown an encirclement of the $(-1, 0)$*, which indicates instability if a secondary feedback controller were to be wrapped around the intrinsic closed-loop temperature control system. There is a significant reduction in the representation in Day 2 and in returning close to nominal behavior of Day 3. The result shows that infectious agents strongly affect temperature control system in putting the body at risk for instability if not handled appropriately.*

predict.

4.1 Verifying Control Law Structure

To assess the assumptions used in deriving the control law and subsequent modeling equations, it is useful to evaluate the model error predicted by the derivation and its ability to fit the data accurately. If the model is overparameterized, then lower order models would be able to fit the data, while if the model is under-parameterized, for example if critical modes are neglected, then higher order models will fit the data dramatically better. As indicated, the model derivation indicates that the temperature dynamics in response to the step function of the case history can be represented as 4 poles and 3 zeros at a nominal operating point. Investigating the model order therefore as a means of evaluating the control law hypothesis, the mean square error of different model orders is presented in Table 4 for each of the trajectories. The (4,3) model performs roughly 7 times better than the (3,2) model, while the (5,4) model is only marginally better at 20% fit; thereby indicating that the (4,3) model is an adequate representation of the data. This trend is the same for Day 2 and Day 3.

Day	(3,2) Model	(4,3) Model	(5,4) Model
1	$8.9\text{x}10^{-2}$	$1.1\text{x}10^{-2}$	$9.1\text{x}10^{-3}$
2	$7.1\text{x}10^{-4}$	$4.7\text{x}10^{-4}$	$2.7\text{x}10^{-4}$
3	$1.6\text{x}10^{-4}$	$7.4\text{x}10^{-5}$	$1.1\text{x}10^{-4}$

Table 4: For a validation of the model structure, the mean square error of the fitted parameter models are compared to the 4 pole, 3 zero structure that was derived. An over parameterized model of 5 poles, 4 zeros, and an under parameterized model of 3 poles, 2 zeros is shown, which indicates that the derived structure provides about 7X enhancement on Day 1 over the under parameterized model, while providing essentially the same predictive quality as the over-parameterized model, thereby indicating an appropriate structure, and some evidence of validation of the modeling approach. Days 2 and 3 produce similar results, although less dramatic since the vaccine is being cleared from the body and thereby inducing less oscillation and transient deviation from nominal.

As an example of the model fitting capability, the confidence band of the standard deviation surrounding the model response for Day 2 is depicted in Figure 7. It indicates that the model does well in capturing the key points of the response which are the breaking points and times associated with the dynamic trajectories of the chill phase followed by a heating and a return to baseline.

To further examine the adequate representation of the system dynamics by the (4,3) model predicted by the derivation, the consequence of the model order is compared in Figure 8 for the fit of Data to the Day 1 trajectory for a model with 3 poles and 2 zeros, and another model with 5 poles and 4 zeros. As seen from the result, the (3,2) model fails to capture an important node of the response, showing a single oscillation, and the (5,4) model falls almost exactly on the (4,3) model, suggesting that the addition of an extra pole and extra zero does not improve the predictive capability. Consequently, it is concluded that a (4,3) model is appropriate model to relate the observed temperature response when subjected to exogenous input in the presence of infections that alter the fundamental dynamic modes.

4.2 Control Law Output

It is of interest to evaluate the control law output which is a function of temperature and the reporter signal concentration, which can be estimated through Equation (57)

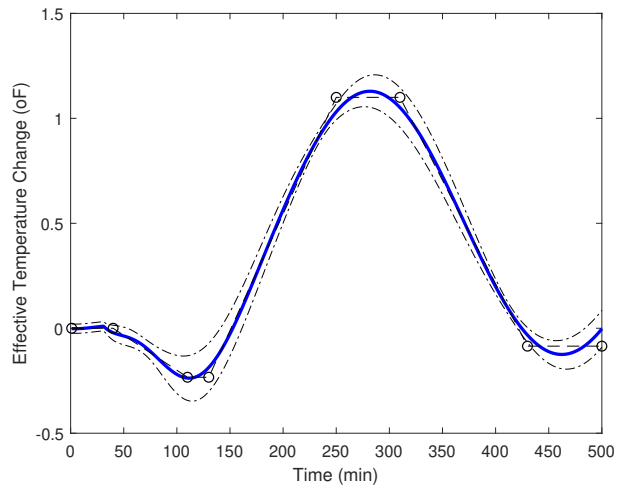

Figure 7: The standard deviation bound is shown for the temperature response of Day 2, indicating tight fitting along the trajectory up and down, with looser fitting during the initial phase of the response and the settling value.

since $G^c_{TE,j}$ has been determined from the temperature response curve. To perform the computation, values for the temperature dynamic term A_T is needed as well as scaling factors W_1 associated with the forcing function, and B_U which scales the control law output signal, $U(s)$. These values can be determined through additional experimentation, however for purposes of this study, estimates are taken as follows: A_T is taken to exhibit a time constant of 3 minutes, which is consistent with the time associated with the body temperature stabilizing to a load disturbance, W_1 is taken as 0.1 scaling, and which passes through as a static gain, particularly influencing the derivative kick of the control law, and B_U is taken as 1, thereby effectively lumping it into the output of the control law. With these values, the control law output is presented in Figure 9, which interestingly has the same general trend as the temperature response, although expected since the model is essentially applies just a first order filter of the control law output. It is noted that the output from Day 1 to Day 3 is significantly different, although the input excitation is the same, thereby indicating further the destabilizing effect of the vaccine for the case study.

4.3 Mediator Signal Estimation

From Equation (60), an estimate of the reporter signal concentration change during the transitional period, although it is necessary to provide first the parameters of the control law of Equation (7). Since information regarding the concentration change of the reporter signal is needed in order to produce the control law parameters, rather a sensitivity study was performed to determine the influence of the control loop parameters on the concentration

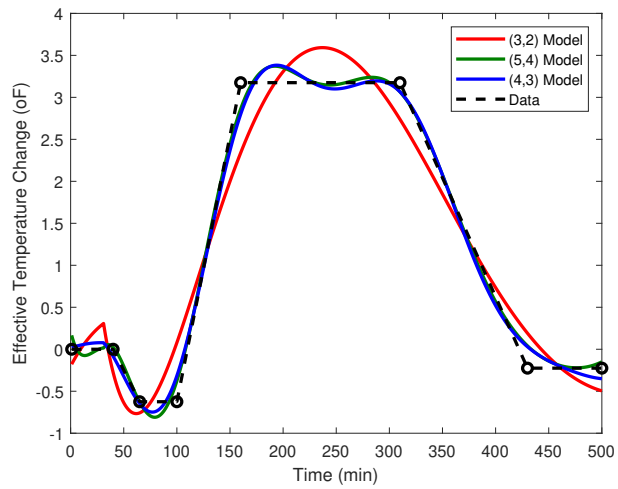

Figure 8: To validate the model structure, a comparison of model order is conducted to see that the data is neither over or under parameterized, which would indicate that response modes are either extraneous or neglected. The comparison is to the 4 poles, 3 zeros model predicted by the derivation to models of the 3 poles, 2 zeros and 5 poles, 4 zeros. The results indicate that 4 poles, 3 zeros is appropriate as characterized by the dynamic trajectory of the first day, which basically coincides with the higher order model, while providing significantly more information than the lower order model, which apparently neglects one oscillatory mode.

of the reporter signal. For the control law of Equation (64),

$$\alpha \Delta U(t) = \left(\Delta T(t) + K_{dT} \frac{d\Delta T(t)}{dt} \right) + \alpha \left(\Delta M(t) + K_{dM} \frac{d\Delta M(t)}{dt} \right) \tag{64}$$

where $\alpha = 1/K_{pT}$, $K_{dT} = 100$, $K_{pM} = 1$ and the derivative term of the concentration, K_{dM} was compared for predicting the reporter signal using the values of 100 and 10, with the scaling factor $\alpha = 1$. The result is shown in Figure 10. The response is shown to be a significantly sensitive to this parameter in shaping the later period stage of the dynamics. It was found that the terms for temperature could be used for the initial part of the response.

In Figure 10, the recurrent theme of highly oscillatory nature of the responses in Day 1, relative to Day 2 and Day 3, when the vaccine had time to clear. The interference with the system dynamics, and the subsequent inefficiencies of the temperature control system are apparent. Thus, the information gathered in response to such excitation is useful in identifying the model equations of the temperature feedback system, which can subsequently be used for further analysis and predictive purposes.

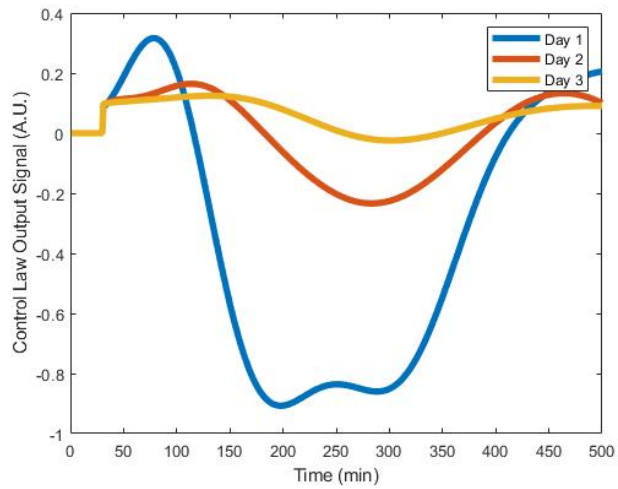

Figure 9: The model is applied to estimate the output signal of the Control Law, Equation (7), using Equation(57). To do so, it is necessary to assign values of the body temperature dyanmics to control input, but that can be done with fairly reasonable guidelines, or can be systematically identified. In this example, a weighting of $W_1 = 0.1$ is selected and a dynamic value of $A_T = 0.3$ is selected, which corresponds to a time constant of 3 minutes, which is consistent with the reported response time of the observed effects of temperature when exercise was ceased of roughly ten minutes, or 3-4 times the extent of the time constant. The output signal, which is sent to the various thermoeffectors, roughly tracks the temperature response shape for this LTI representation, and therefore this signature can aid in the identification of the neurological signals comprising the control law function.

4.4 Influence of infectious agent on temperature dynamics

As noted from the analysis of the transient and spectral characteristics of the identified models for Days 1, 2, and 3, the vaccine has a significant influence on the temperature response when stressed, and the fundamental nature proposed is the interference of the vaccine molecule in its interaction with the reporter signal molecule. Further, as noted in Figure 11, which represents a relation of the differences of the amplitude and phase between the response associated with Days 1 and 2, the differences are due not only to the reaction kinetics of the reporter signal, Equation (15), but also the dynamics associated with the vaccine depletion, Equation (33). Had it only been due to the reporter signal reaction rate, the difference in model structure would have been in examining Equation (52) a constant amplitude of $1/\bar{D}_M$ and a phase associated with the time delay; however, the response is more complex indicating the participation of each element associated with the interaction between vaccine and reporter signal. The transition from Day 1 to Day 2 for the two LTI representations, has break points at 0.01 rad/min and 0.04 rad/min, corresponding to time constants of 100 minutes and 25 minutes, or roughly 5 hour and 1 hour response periods.

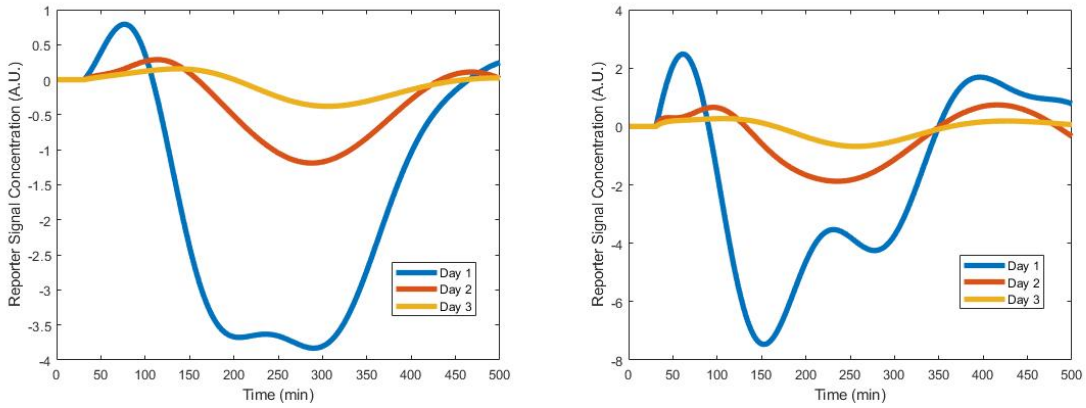

(a) $K_{dM} = 100$ (b) $K_{dM} = 10$

Figure 10: Through the use of the model the trajectory of the mediator, or reporter signal, that is mapped to the cardiovascular system status, can be estimated. Two values of the PD control law are evaluated for different values of the derivative term of the mediator, with the other values of the controller kept constant at $K_{pT} = 1$, $K_{dT} = 100$, and $K_{pM} = 1$. It is seen that the shape of the concentration of the mediator follows along the lines of the observed temperature response but can be shifted in the later response stage by the derivative action. Although not shown, a similar effect is seen in the earlier stage of the response by altering K_{dT}. Thus, the mediator should have a trajectory correlated to the temperature response.

4.5 Minimizing Temperature Fluctuations

One question that can be assessed using the model response is whether the observed temperature fluctuations of the case study due to the abrupt cessation of exercise would have been reduced had there been an extended cool down period in which the exercise was gradually reduced. This would seem to be the case since the frequency response of the closed-loop model indicates certain peaks which if excited would result in larger oscillatory responses, and therefore if the excitation can be kept to low frequencies, then less peak temperature fluctuation should be expected. This turns out to be the case, as seen in Figure 12, which compares the temperature fluctuation observed for Day 2, when the exercise was immediately stopped, in comparison to the temperature fluctuation had the exercise been gradually ramped down for the full period of observed nominal temperature oscillation. It is noted that temperature deviations during the exercise period were not observed because it was slow relative to the cessation of the exercise, and hence essentially a ramp, which can be modeled as $1/s^2$ that has significantly more frequency roll-off and attenuation then the step response of $1/s$.

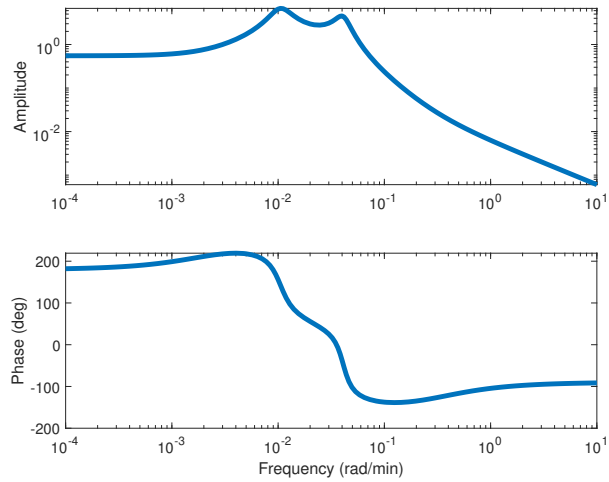

Figure 11: To assess the transition in model dynamics as the vaccine is cleared from the body due to phagocytosis and other mechanisms, the difference of the frequency response is examined for the models of Day 1 and Day 2, which indicates that the resonant peaks at time constants of approximately 100 minutes and 25 minutes, resulting in expected in how the body temperature will respond in both short term and long term, roughly 5 hour and 1 hour response periods.

4.6 Cooperating Interactive Control Loops: Cardiovascular and Nervous Systems

A very interesting consequence of the proposed control law mechanism is an intersection of signals associated with the cardiovascular system, that is the reporter signal $M(s)$, and with the nervous system, that is the neurological connections associated with the thermoreceptors sensing temperature $T(s)$ and its fluctuations. The intersection is indicated in Figure 13 with the disturbances induced from external sources, $\mathbf{E}(s)$. The inputs to the control law, whose location is assumed to be the hypothalamus region, are chemical and electrical in nature, and the output of the control law is electrical (neurologic). Note that the block diagram, which nicely compartmentalizes the immune response with the cardiovascular and nervous system, is formulated as a graphical representation of the mathematical equations describing the process. This is intriguing because it clearly would indicate how the overall system works with precise mathematical terms. In comparison, in other research on temperature control, such feedback schematics are described by words, whereas this has a mathematical basis, enabling quantitative analysis and predictions.

The control loops are cooperative in the sense that stressors placed on the cardiovascular system, such as increased oxygen demand, can be balanced by the requisite temperature response. And conversely, stressors placed on the temperature, such as the need to dissipate heat, can be balanced by the circulatory response, such as with vasomotor activity whose

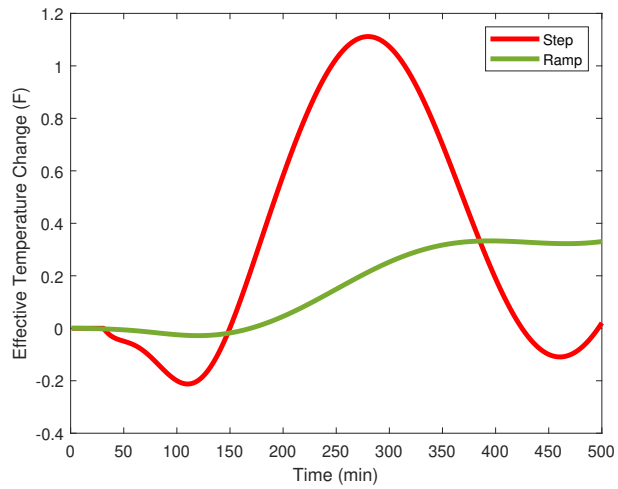

Figure 12: The model has predictive capability in optimizing and planning voluntary activity to compensate for sub-optimal situations. In this example, the temperature deviations are minimized if the cool down period after exercise were to have been conducted over an extended period, represented as a slow ramp down in activity, relative to just stopping the exercise regime, represented as step-down in the case study. The slow ramp down avoids the excitation of resonant frequencies in the dynamic response, which are present due to the vaccination altering the inherent dynamic response, pushing the system closer to instability in inducing oscillatory temperature modes.

extent is measured by a circulating reporter signal, $M(s)$. Conversely, the control loops are not run independently, in that changes made to the cardiovascular system are conducted in conjunction with the temperature regulation system.

4.7 Other Insights

The mathematical representation enables several insights into temperature control, including providing answers to questions of general interest, as follows:

- **Fevers:** To address a common debate on whether a fever is *good or bad*: this analysis indicates that fevers are a consequence of the dynamics associated with the temperature control laws and interactive loops of relatively high dynamic gains. It is mathematically inevitable given the high gain construct of the temperature control law that there is sub-optimal operation due to a shift in parameters governing the dynamics. In industrial process control, it is well known that high gain systems are high performance but are susceptible to shifts in the dynamics of the operation, in which performance rapidly degrades, or even becomes unstable [27]. As noted in medical physiology textbooks [17], the feedback gain (the ratio of the change in

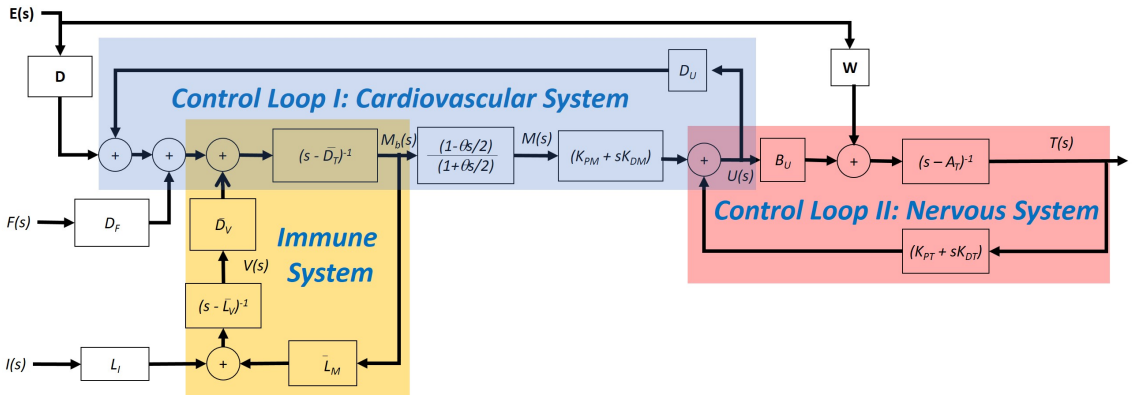

Figure 13: The schematic of the feedback control law and model of Figure 3 is partitioned to indicate interactive and cooperative control loops of the cardiovascular system and the nervous system, as well as the inputs via the immune system into the cardiovascular system. Note the cooperation of the cardiovascular and nervous system, as for example, the cardiovascular system responds to commands, for example from the need for increased cellular oxygen due to sympathetic stimulation, the nervous system will respond automatically by feedback control to regulate temperature, thereby maintaining a homeostatic internal environment. The converse in cooperative feedback loops holds as well, for example with external temperature disturbances, due for example to an increase in external environmental temperature, are automatically compensated by the feedback controller of the cardiovascular system through the control law of Equation 7.

environmental conditions to the change in body temperature) for body temperature averages 27, "extremely high for a biological control system"; (for comparison, the baroreceptor arterial pressure controller is less than 2.) Thus, sources inducing fever may arise from the two coupled systems: (a) cardiovascular system - external agents that directly interfere and react with the reporter signal molecules $M(s)$ thereby altering the control law response and loop coordination thus compromising the performance of the temperature control laws, Loop I in Figure 13; (b) nervous system - external loads placed on the system from neural pathways, including psychosomatic and sympathetic stressors, or agents that stimulate that drive the temperature response, Loop II in Figure 13. Therefore, it is proposed through this model that fevers are not in place fundamentally as somehow beneficial to fight infections, but rather are an unfortunate side effect of a high performance temperature control system that is tuned for optimal operation at nominal circumstances, essentially a control system that trades off robustness for very high performance at usual conditions. Additional arguments based on evolutionary factors as to why optimal temperature performance would be needed during high stress situations, such as those associated with sympathetic responses of flight or fright, can be made for this analysis.

- **Chills preceding Fevers:** The rather odd response of a chill preceding a fever can be explained in the model structure as due to the non-minimum phase nature of the closed-loop feedback control system. For the model order of this response, which has four poles and three zeros, rather slight alterations in the locations of these roots can induce a so-called inverse response as well as produce oscillations in temperature response, an indicator that the system is driven closer to instability. Essentially, the loss of coordination between the circulatory and neurologic system responses, due to an infectious agent for example, results in the observed inverse response and other such wrong-way, or illogical, control actions. Non-minimum phase systems are common in chemical process control, and even aerospace control, and to eliminate inverse response would require a re-design of the overall control architecture [13]; however, it is the case that higher performance under nominal loads can be achieved, but the drawback is instabilities in open-loop. Under feedback control, however the loop is stabilized and high performance results. However, the system is sensitive to plant degradation from the nominal configuration, and performance can be greatly compromised, which has been noted in the frequency response analysis of the case history of Section 2.

- **Challenges in Thermoregulation Research due to Coupling and Dynamics:** As an area of research, thermoregulation is challenging for reasons as identified by the block diagram of 13, in which the systems of the cardiovascular and nervous are coupled to initiate a combined effect. Thus dynamics are critical to the analysis to identify the appropriate mapping of cause and effect. Further, disturbances from exogenous disturbances, including stress, can alter the observation as it is another input source other than then one that may be under study. Further, *a priori* conditions are important, as the dynamics of past stimulation take time to settle before the analysis can begin. As such, temperature effects arise from many sources [2], and thus, establishing causality is a complex process, which the aid of a guiding top-down integrative model as this research provides is needed. (It is noted that in the model development for the system, additional coupling of the temperature effects of the kinetic parameters of the cardiovascular and immune systems could have been incorporated in the linearization steps for $V(s)$ and $M_b(s)$, which would have resulted in additional complexity in the analysis, but the simplicity of the model derived can enable insights into detailed evaluation of molecular mechanisms, such as additional evaluation of the reporter signal $M_b(s)$.)

- **Consistency as Model Validation:** To further validate the modeling approach and derived control law, it is noted that the model predictions are consistent with anecdotal information, for example: (1) as noted on www.elite-cryo.com, a cryotherapy session can not be used if the client is sick (common cold, flu, etc.) and the client must be free of a fever for at least 48 hours, which is consistent with our finding that the temperature response is greatly compromised when subjected to infectious agents

and external shocks in temperature can have significant consequences; (2) Aspirin is often linked as an anti-pyretic molecule, and this can be explained in the model as an external feed $F(s)$ of Equation (44) of its interaction in mimicking the reporter signal molecule which would compensate for the loss of reporter molecule due to the vaccine and aid in smoothing the temperature profile. Under nominal conditions, aspirin would have little impact on body temperature since the temperature control system is operating at optimal conditions and the coupled control loops could compensate for the load in the cardiovascular loop due to $F(s)$; (3) the model includes the possibility of linking amphetamine induced or alcohol-withdrawal fevers, which can alter the sympathetic nervous system, thereby causing a loss of coordination with the circulatory system and inducing fevers: these would enter the model Equation (44) through the exogenous disturbance vector $\mathbf{E}(s)$; (4) the findings indicate that temperature shocks induce large temperature dynamics due to excitation of resonant frequencies of the dynamic response curve, which is consistent with the reports that trying to place someone with a fever in an ice-bath is not an appropriate action as it can have deleterious effects.

- **Feedforward, Supervisory, and Behavioral Control:** Based on the model, temperature control is predominantly performed by feedback-only methods, effectively proportional-derivative action. It was noted in evaluation of the Nyquist curve Figure 6 that for a secondary loop wrapped around the internal feedback control loop could result in instability if implemented on the same time scale as the autonomic temperature control system when destabilized by an infectious agent, for example. But feedforward does have a role to play however if performed on a slow time scale without direct interaction with the temperature output, would not necessarily destabilize the closed-loop control loop system, and could be implemented in a cerebral context, for example putting on a jacket, or shedding clothes to control heat. These actions would enter the model through $\mathbf{E}_j(s)$ with weighting of W_j in scale of the input acting as a forcing function via the skin temperature, and with $D_j = 0$, since it would not directly interact with the reporter signal molecular of the cardiovascular system. Thought processes in which conscious patterns can elicit a fever response would be incorporated in the model through $E_j(s)$, $D_j \neq 0$, and $W_j = 0$, which would trigger a response in $M_b(s)$ that would be offset by responses in $T(s)$. Note however that in this situation the internal dynamics are unaffected by the thought patterns, and therefore a stable response is expected.

- **Setpoint:** A variable "temperature setpoint", which is utilized in historical and current explanations of thermoregulation, is not required by the control law of this paper, of which body temperature dynamics are derived as deviation variables about static conditions and similarly the term reflecting the rate of change, that is the time derivative also does not have a set-point other than a nominal value of zero. In addition, a concentration setpoint of the reporter signal is also not required, just

its deviation and its rate of change. Thus, it is a conclusion of this analysis that variable set-points with respect to temperature do not exist, and body temperature merely fluctuates about a static nominal value under high gain feedback control. The nominal value is therefore largely set-up at birth, remains constant although shifting slightly higher from infancy to adulthood. Body temperature is established as it acts in conjunction with the cardiovascular system in mutually equilibrium at values in proportion to the nuero-junctions of $M(s)$ and $T(s)$, which are used by the control law to produce the control signal $U(s)$.

- **Exercise:** The role of exercise in this study is important as it mimics a sudden need for vasodilation in fight or fright situation, and thus can be used to stimulate the body temperature due to its coupling with the cardiovascular system. Thus, as proposed in the theory, the balancing between the cardiovascular system and the nervous system to control temperature is highlighted. When a demand for oxygen is needed, due to the coupling at the control law, the temperature will automatically be balanced accordingly (and vice versa) Therefore, in the study of thermoregulation, exercise is an excellent method of study since it stimulates the cardiovascular system in a predictable manner, and changes in the temperature response may be modeled effectively. It has been noted that exercise offers insights into bottoms-up analysis of temperature [20], and it is valid in this top-down approach. By systematically creating a chemical imbalance in the cardiovascular system, and stimulating the effect of the imbalance through an exercise regimen, its response can be evaluated and causality established through the aid of the model provided by this research. The exercise regime should be routine and practiced many days in advance to make it a normal occurrence in order to isolate the effects of the exogeneous stressor.

- **Highly challenging nature of infectious agents:** This paper highlights that infections $V(s)$ enter the temperature dynamics through adjustments to the poles of the closed-loop temperature dynamics whereas exogeneous stressors $E(s)$ and even chemical inputs $F(s)$ do not affect the poles, but rather the zeros and gains of the system, that is the shape of the response, rather than the fundamental nature of the temperature response, which can lead to instability. While changes to $E(s)$ and $F(s)$ can be controlled if there is sufficient control authority, the response due to $V(s)$ may lead to unstable behavior, even if there is sufficient control authority to counteract the effect because of the fundamental adjustment to the dynamic modes induced by the infectious agent.

4.8 Comparison with Current Theories of Thermoregulation

As described in the recent article heading a collection of research chapters on thermoregulation [24], theories of thermoregulation can tbe grouped into two categories: one historical

that involved changes to a temperature setpoint and one more recent that includes a series of feedforward loops to describe temperature effects.

The theory on temperature setpoint, as indicated in Section 1 which is standard fare in medical physiology textbooks, suppose that a temperature setpoint is adjusted in the hypothalamus, and that the body will therefore enter a hypothermia phase, where it will "feel" cold, followed by a hyperthermia phase where it will be in a fever condition. However, this theory offers little in quantitative maps that can predict temperature trajectories, as seen in the theory in this paper. Moreover, the theory of a temperature setpoint would not be able to explain the results of the present study, that is, if the infectious agent had actually changed the temperature setpoint, why would it change only after the exercise period was completed, and not while the exercise was being conducted? How does it know when to decrease the temperature setpoint back to baseline and why would it change the temperature setpoint less the second and third days? There is no quantitative framework from which to analyze the temperature trajectories, and thus can not be compared in an analytic way to the mathematical relations developed in this paper. Further, there is no anatomical experimental evidence of a temperature setpoint [24].

The newer theories on temperature regulation do not require setpoints but rather use zones and feedforward loops to explain temperature effects. A quantitative framework however is lacking in the framework from which to produce temperature predictions from exogenous stressors. Moreover, in [24], the last paragraph of the paper indicates that there are fluctuations in temperature, particularly those in regard to exercise, in which it is only at a hypothesis of evaluation in terms of fitting within the overall framework, which is still in development. Because the theory is under construction, and because there is no clear quantitative model, it is not possible to analytical examine the proposed theory. In addition, it would be difficult to determine how feedforward control could be incorporated in the results: how much feedforward would be determined, and why would it be implemented in response to the pneumococcal vaccine. Moreover, as pointed out in the paper, the closed-loop response due to infectious agents can exhibit an unstable if excited at the appropriate frequencies, and thus if feedforward action on a rapid scale were to be implemented, the fever response could be often unstable. However, the proposed theory is agreement with the newer theories of thermoregulation in that it does not require the previous concept of a temperature setpoint.

The proposed theory of this paper introduces a chemical signal in coordination with a neural signal to explain temperature responses deploying feedback only control, whereas the other theories using only a neural signal to explain temperature control. The approach of this paper is consistent with other functions that utilize neurochemical signals to affect the outcome in a feedback-only mechanism. For example, fMRI (functional magnetic resonance imaging) signals deploy a model explanation in which oxygen acts as a controlling factor in neurological signals. By introducing a chemical signal, it was clear how external chemical species generate a response in temperature, whereas in the other theories of setpoint or feedforward control, it is not quantitatively clear. It is noted that the block diagram of

Figure 13 is mathematically very precise, whereas the alternative theories generally use words to describe the effects, thus lack analytic use.

4.9 Future Directions

A mathematical model describing an individual's temperature dynamics in response to exogenous factors, including infectious agents, would be quite useful, as it could be used for monitoring one's health in comparison to nominal performance, and could be used to suggest appropriate actions, such as how to regulate one's activities when the temperature control loops are compromised, or how the body would respond to anti-fever medications or the side effect of temperature response to medications, such as vaccinations. To improve upon the techniques described in the paper, additional temperature response data can more fully characterize the dynamics, such as the model on body temperature, which can be obtained with a specific set of input excitations and response data. The reaction kinetics of agents in and reporter signal molecule could be more fully characterized to describe other reaction orders and interactions. Instead of a multiple set of LTI models to characterize the nonlinear phenomena, a model incorporating the nonlinear nature could be developed. While a reaction kinetics associated with prostaglandins or nitric oxide seems to be likely, the identification of the reporter signal molecule should be further examined and identified. In addition to the chemical pathways, the neurological pathways transmitting the control output could be mapped and the various gains established. Other areas include mechanisms of controlling temperature by chemical methods, such as chemicals that mimic the signaling molecule and how to predict whether one is starting to get affected by viruses, bacteria, from the temperature response, and what type of pathogen based on the internal temperature response and dynamics. The use of the model in vaccine development would also be useful, and in developing optimal protocols to reduce heat shock effects when rapid reduction in temperature is needed.Moreover, the implementation of a control law similar to that of body temperature, that is as a function of chemical and neural signals associated with the cardiovascular system and the nervous system, to other symptomatic responses influenced by infectious agents appears to be similar, including cardiopulmonary and inherent neural responses.

4.10 Summary of Main Findings

1. A chemical signal associated with the cardiovascular system, that interacts with a neural signal in the central nervous system, are together responsible for the observed dynamics of body temperature control.

2. An internal control law can model the link of the cardiovascular and nervous system to produce a neural command of the thermoeffectors for thermoregulation in response to neurochemical signals.

3. The internal control law is a function of both the magnitude and the rate of change of the cardiovascular and neural signals, in which the rate of change is determined from the spatial gradient of the signals modulating the signal strength of the CNS response.

4. The interaction of infectious agents with the cardiovascular chemical signal component explains thermoregulation effects, indicating that a modification of the fundamental dynamic modes, that is the poles, of the temperature dynamic mapping, which is quite serious situation.

5. Incorporated exogeneous stressors into the dynamic equations, mainly as input sources to the cardiovascular signal component, produce a less serious situation than that of an infectious agent, since the fundamental dynamic modes are unaffected, just the dynamic zeros.

6. A closed-loop model of temperature effects, including the output signals from the control law, naturally led to a mathematically precise graphical representation of the interaction of the immune system, cardiovascular system and the nervous system.

7. A routine exercise protocol was developed that can be used to study temperature effects in which nominal vaccination is used as the triggering point.

8. The mathematical formulation drew several insights and new explanations of fever (mathematically inevitable as a robustness tradeoff for performance at nominal conditions), chills preceding fever (which is caused by the alteration of the dynamic modes due to the infectious agent),

9. A feedback-only temperature control law was used to explain temperature effects, thus providing a simpler yet more powerful analytic description of temperature control than the current theories of feedforward control and of temperature setpoints, of which an inherent temperature setpoint was not needed in the new model.

10. A framework was provided to make temperature predictions and quantitative analysis, which can be generated from a sparse set of temperature response data, therefore making it accessible to many potential participants.

5 Conclusions

A mathematical model is developed for the first time that includes a chemical signal and a neural signal to describe body temperature dynamics, which thereby coordinated cardiovascular and neural pathways. Moreover, only feedback control loops about a nominal operating point were utilized in the computational description, thus precluding the use of a temperature setpoint changes as well as feedforward loops, both of which are required

in other theories of body temperature control. Further, the pathways by which infectious agents attack body temperature control are shown in a quantified framework, as well as the analytical impact of other exogenous stressors. In an evaluation of a case study, the resultant closed-loop model described observable temperature responses to a routine exercise protocol over a multiple day period, which also brought to light the significant effects on internal body temperature dynamics of significantly degraded thermoregulatory performance from infectious agents , as assessed by the analysis of the frequency response and stability of the temperature control system. In addition, the proposed model was used in an analysis to characterize odd temperature responses of chills preceding fevers, as well as the oscillatory nature of temperature control. For the first time, fever was shown to be simply a by-product of the feedback control law designed for high performance at nominal conditions, thereby trading off robustness, and thus exhibiting sensitivity at certain resonance modes due to infectious agents disrupting the internal model characteristics through its interaction with a cardiovascular signaling species. Further, to reduce temperature variations when infected, the model provided guidance in designing optimal plans for cool-down procedures following physical activity. In addition, the model was linked to other potential inputs to the temperature control system, including externally introduced chemical streams that do not alter the inherent system dynamic relations, as well as other inputs that stimulate the sympathetic nervous system. Because temperature responses to infectious agents and other causal factors are now well characterized by the new mathematical description, the model should provide a unifying framework from which to analyze, predict, and study body temperature dynamics and responses.

Bibliography

[1] LA Abdulkhaleq, MA Assi, Rasedee Abdullah, M Zamri-Saad, YH Taufiq-Yap, and MNM Hezmee. The crucial roles of inflammatory mediators in inflammation: A review. *Veterinary world*, 11(5):627, 2018.

[2] Thomas E Andreoli, J Gregory Fitz, Ivor Benjamin, Robert C Griggs, and Edward J Wing. *Andreoli and Carpenter's Cecil Essentials of Medicine*. Esevier Health Sciences, 2010.

[3] Ask the Experts. What causes fever. *Scientific American*, (2), 2006.

[4] Abolhassan Behrouzvaziri. *Thermoregulatory Effects of Psychostimulants and Exercise: Data-driven Modeling and Analysis*. PhD thesis, 2018.

[5] Anders Blomqvist and David Engblom. Neural mechanisms of inflammation-induced fever. *The Neuroscientist*, page 1073, 2018.

[6] Christian Bogdan. Nitric oxide synthase in innate and adaptive immunity: an update. *Trends in immunology*, 36(3):161–178, 2015.

[7] Sebastian Boltana, Nataly Sanhueza, Andrea Donoso, Andrea Aguilar, Diego Crespo, Daniela Vergara, Gabriel Arriagada, Byron Morales-Lange, Luis Mercado, Sonia Rey, et al. The expression of trpv channels, prostaglandin e2 and pro-inflammatory cytokines during behavioural fever in fish. *Brain, behavior, and immunity*, 2018.

[8] Stephen Boyd and Craig Barratt. Linear controller design: limits of performance. Technical report, Stanford University Stanford, CA, 1991.

[9] Vittorio Calabrese, Cesare Mancuso, Menotti Calvani, Enrico Rizzarelli, D Allan Butterfield, and Anna Maria Giuffrida Stella. Nitric oxide in the central nervous system: neuroprotection versus neurotoxicity. *Nature Reviews Neuroscience*, 8(10):766, 2007.

[10] Charlotte Farah, Lauriane YM Michel, and Jean-Luc Balligand. Nitric oxide signalling in cardiovascular health and disease. *Nature Reviews Cardiology*, 15(5):292, 2018.

[11] Fever. Fever — Wikipedia, the free encyclopedia, 2018. [Online; accessed 28 - November - 2018].

[12] CE Fields and RG Makhoul. Vasomotor tone and the role of nitric oxide. In *Seminars in vascular surgery*, volume 11, pages 181–192, 1998.

[13] Gene F Franklin, J David Powell, and Abbas Enami-Naeini. *Feedback control of dynamic systems*. Addison-Wesley, Reading, MA, 1994.

[14] Andras Garami, Alexandre A Steiner, and Andrej A Romanovsky. Fever and hypothermia in systemic inflammation. In *Handbook of Clinical Neurology*, volume 157, pages 565–597. Elsevier, 2018.

[15] Bruna Rafaela Bezerra Gomes, Natália Carvalho Guimarães, Gabriela Luna Soares de Sousa, Débora de Sousa Alves, Marcelo Valle de Sousa, Paulo Eduardo Narcizo de Souza, and Fabiane Veiga-Souza. Electron paramagnetic resonance detection of nitric oxide produced in different tissues during fever and antipyresis. *Free Radical Biology and Medicine*, 128:S112, 2018.

[16] Alexander V Gourine. Pharmacological evidence that nitric oxide can act as an endogenous antipyretic factor in endotoxin-induced fever in rabbits. *General pharmacology*, 26(4):835–841, 1995.

[17] John E Hall. *Guyton and Hall textbook of medical physiology*. Elsevier Health Sciences, 2015.

[18] Thomas Kailath. *Linear systems*. Prentice-Hall Englewood Cliffs, NJ, 1980.

[19] Lennart Ljung. *System identification: theory for the user*. Prentice-hall, 1987.

[20] Milene R Malheiros-Lima, Washington Pires, Ivana AT Fonseca, Julliane V Joviano-Santos, Anderson J Ferreira, Cândido C Coimbra, Nilo RV Lima, and Samuel P Wanner. Physical exercise-induced cardiovascular and thermoregulatory adjustments are impaired in rats subjected to cutaneous artery denervation. *Frontiers in physiology*, 9:74, 2018.

[21] SF Morrison and K Nakamura. Central mechanisms for thermoregulation. *Annual review of physiology*, (0), 2018.

[22] Kei Nagashima, Ken Tokizawa, and Shuri Marui. Thermal comfort. In *Handbook of Clinical Neurology*, volume 156, pages 249–260. Elsevier, 2018.

[23] Andrej A Romanovsky, editor. *Thermoregulation: From Basic Neuroscience to Clinical Neurology*. Elsevier, 2018.

[24] Andrej A Romanovsky. The thermoregulation system and how it works. In *Handbook of Clinical Neurology*, volume 156, pages 3–43. Elsevier, 2018.

[25] Joachim Roth, Birgit Störr, Karlheinz Voigt, and Eugen Zeisberger. Inhibition of nitric oxide synthase attenuates lipopolysaccharide-induced fever without reduction of circulating cytokines in guinea-pigs. *Pflügers Archiv*, 436(6):858–862, 1998.

[26] Thomas E Scammell, Joel K Elmquist, and Clifford B Saper. Inhibition of nitric oxide synthase produces hypothermia and depresses lipopolysaccharide fever. *American Journal of Physiology-Regulatory, Integrative and Comparative Physiology*, 271(2):R333–R338, 1996.

[27] Dale E Seborg, Duncan A Mellichamp, Thomas F Edgar, and Francis J Doyle III. *Process dynamics and control*. John Wiley & Sons, 2010.

[28] George Stephanopoulos. *Chemical process control*. Prentice-Hall Englewood Cliffs, NJ, 1984.

[29] Chan Lek Tan and Zachary A Knight. Regulation of body temperature by the nervous system. *Neuron*, 98(1):31–48, 2018.

[30] Tun-Linn Thein, Joshua Wong, Yee-Sin Leo, Eng-Eong Ooi, David Lye, and Tsin W Yeo. Association between increased vascular nitric oxide bioavailability and progression to dengue hemorrhagic fever in adults. *The Journal of infectious diseases*, 212(5):711–714, 2015.

[31] John R Wilson and Shiv C Kapoor. Contribution of prostaglandins to exercise-induced vasodilation in humans. *American Journal of Physiology-Heart and Circulatory Physiology*, 265(1):H171–H175, 1993.